Project funded by EUROPEAN UNION

PONTOS

Black Sea CROSS BORDER COOPERATION

Copernicus assisted environmental monitoring across the Black Sea Basin – PONTOS

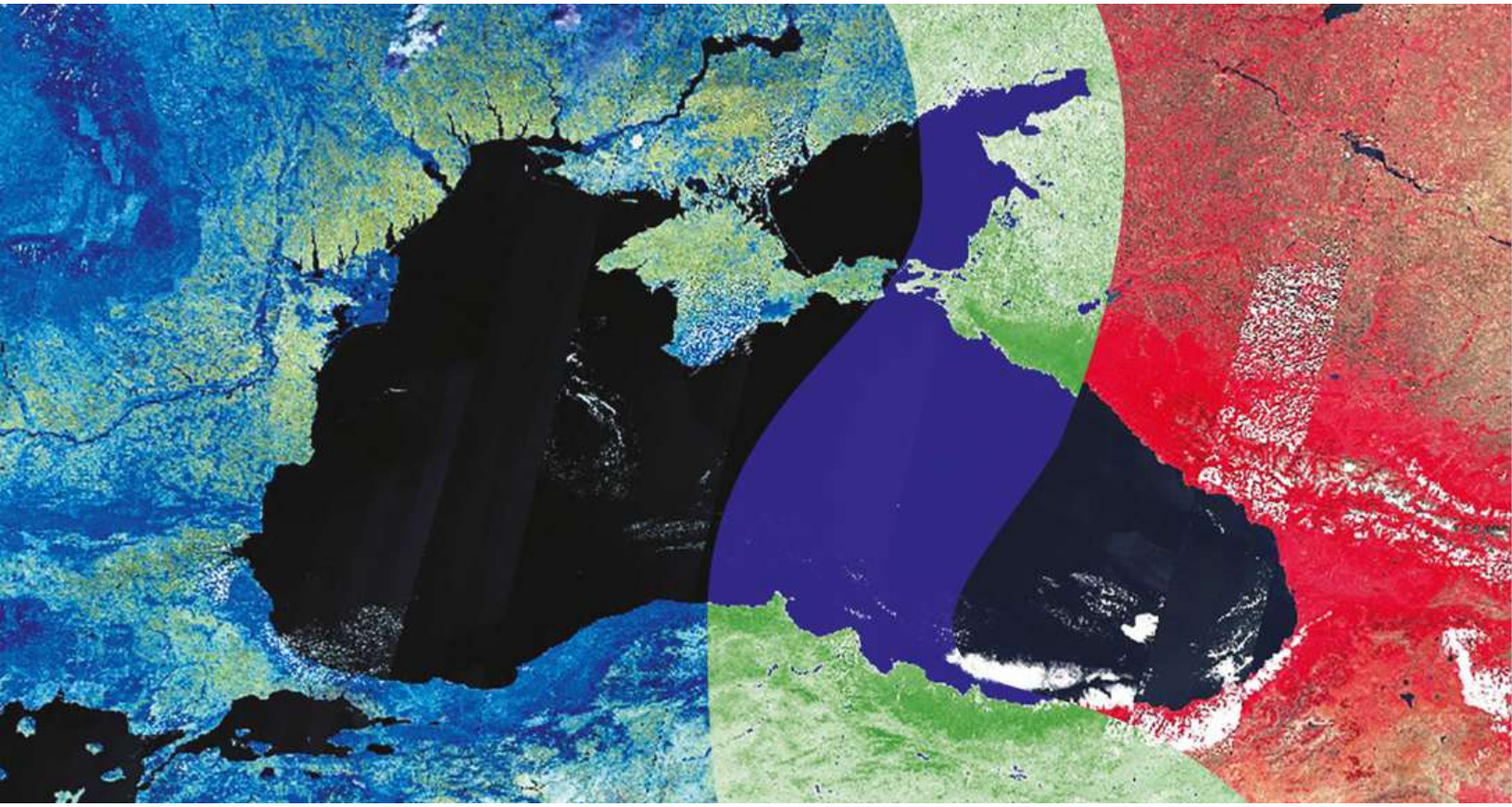

Assessment on changes in wetland and floating vegetation cover

Technical Report

Prepared by Artak Piloyan

PONTOS-AM

Sevan Lake and its catchment area

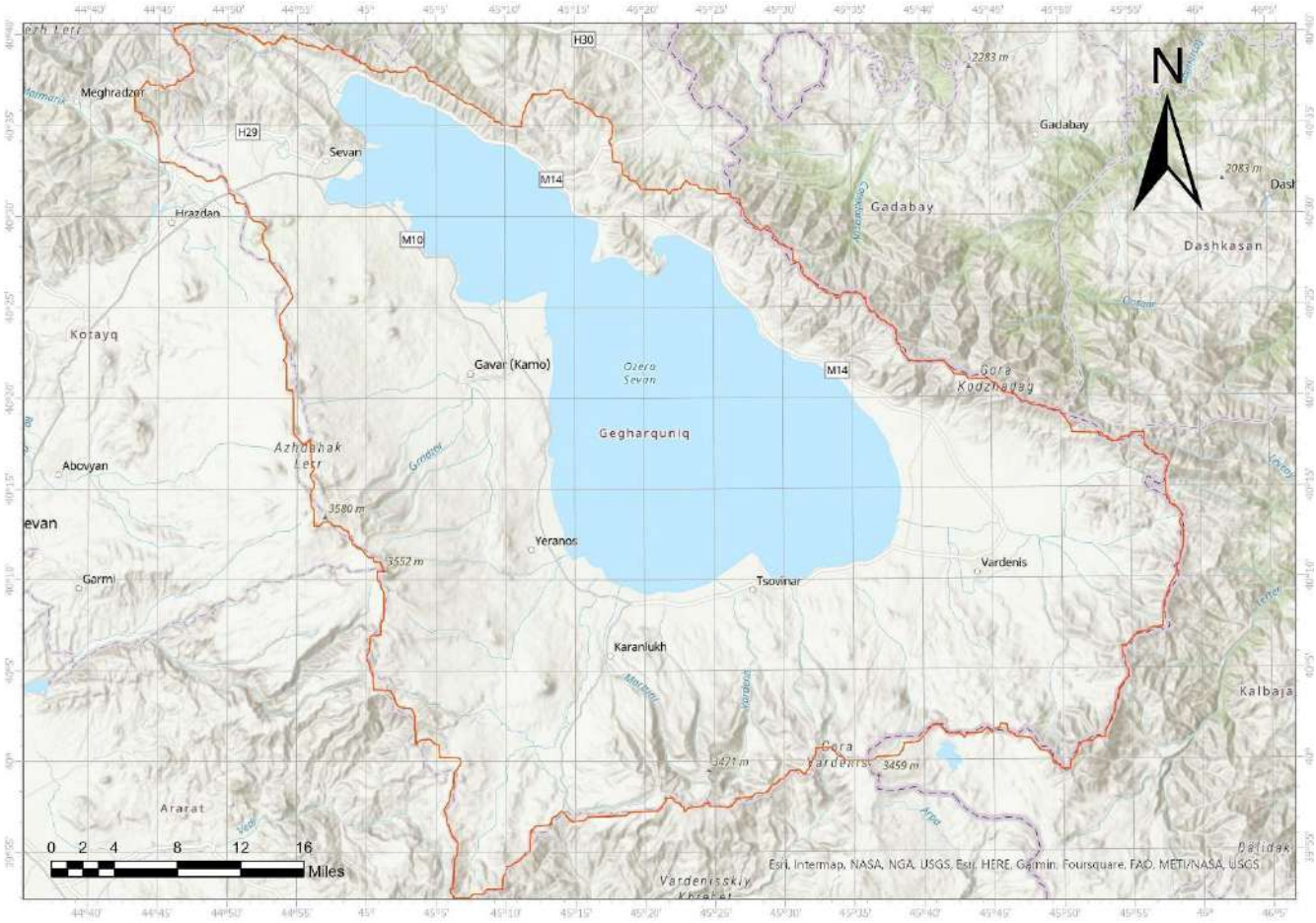

Table of Contents

1. Introduction and Background

Aquatic vegetation is a diverse group of photosynthetic organisms that grow permanently or periodically in wetlands, the shoreline of lakes and along streams (Seddon, 1972; Junk and Howard-Willams, 1984; Alahuhta et al., 2012; Chappuis et al., 2014). They are a natural part of every lake ecosystem and serve many purposes in a lake, can help the migration and circulation of elements, purify water quality, and limit the growth of algae (Ou et al., 2008). They are an integral part of aquatic ecosystems and play an important role in immobilizing pollutants, regulating oxygen production and global carbon cycle, stabilizing sediments and protecting shore erosion (Engelhardt and Ritchie, 2001; La Toya et al., 2013; Chappuis et al., 2014).

Aquatic vegetation can be classified into four functional groups as emergent (EAV), floating-leaved (FAV) and rooted, free-floating, and submerged (SAV), based on their growth form, morphology, and adaptation to the environment (Chambers et al., 2007; 9. Thomaz et al., 2009). Figures 1 and 2 show two classification schemes for aquatic vegetation types.

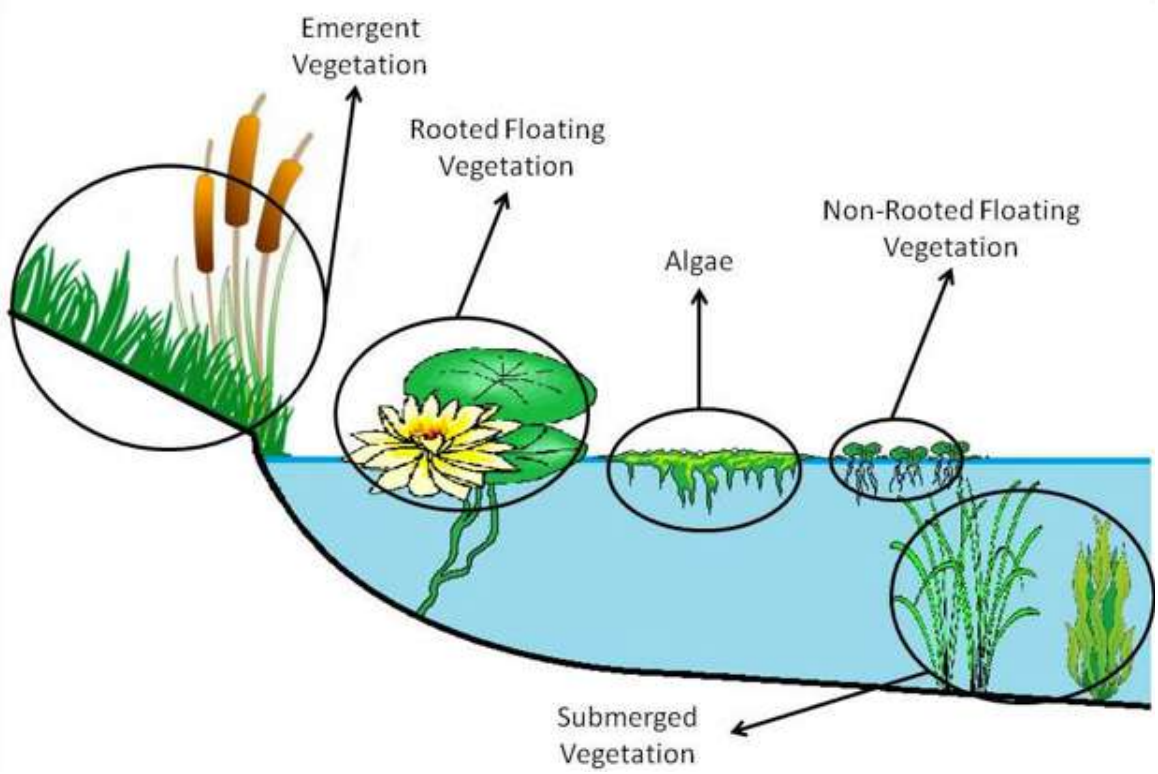

Figure 1: Classification of different types of aquatic vegetation (variant 1) [source: https://fw.ky.gov/Fish/Pages/Farm-Pond-Management-Vegetation-Control.aspx]

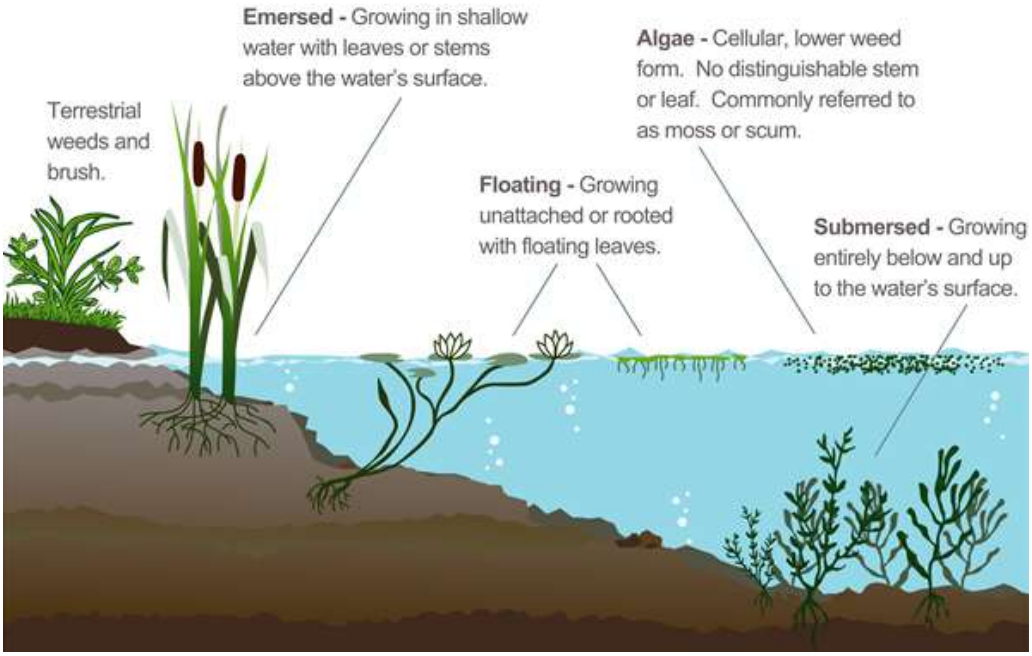

Figure 2: Classification of different types of aquatic vegetation (variant 2) [source: http://invasivespecies.ie/invasive-plants-japanese-knotweed/aquatic-weeds/]

The impact of anthropogenic stressors and climate change on water-level and aquatic vegetation has been evident in recent decades. The interaction between anthropogenic stressors, land-use change, and water-level variability affects aquatic macrophytes to a great extent (Damtew et al. 2021).

Therefore, it plays a critical role in protecting the biodiversity and ecological balance of freshwater ecosystems such as lakes and rivers (Fernandes et al., 2013).

Distribution and composition of macrophyte communities are influenced by nutrient load, and climatic and hydrological conditions such as spatial and temporal variations of water level (Chappuis et al., 2014; Van Geest et al., 2005; Zhu et al., 2019; Tan et al., 2020). Lake water level changes provide an opening for seedling recruitment for perennial emergent aquatic plants (Lawniczak et al. 2010; Triest et al., 2014). On the contrary, a low water level causes succession and terrestrialization of aquatic ecosystems (Dolinar et al., 2016; Luo et al., 2016). Climatic conditions such as temperature and rainfall fluctuations also affect germination rates of aquatic vegetation (Chappuis et al., 2014; Zhang et al., 2016).

Timely recording and mapping of spatio-temporal distribution and composition of macrophytes is necessary to understand factors which influence distribution and composition of macrophytes (Hunter et al. 2010; Burlakoti and Karmacharya, 2004). Conventional field survey approaches

for macrophyte monitoring can give good estimates and provide reliable and reproducible taxonomic information (Birk et al., 2014; García-Girón et al., 2019; Lindholm et al., 2020). However, these methods cannot capture whole-lake macrophyte cover or their patchy distribution and are hindered by technical and logistical limitations (Vis et al., 2003; Beck et al., 2010). Alternative approaches such as remote sensing techniques and the use of satellite imagery can provide data covering large areas in space and time (Hunter et al., 2010; Albright and Ode, 2011; Jiang et al., 2012).

Different remote sensing techniques have been developed to systematize the identification and change detection of aquatic vegetation from satellite data (Jakubauskas et al., 2000; Rivera et al., 2013; Villa et al., 2015) and recent advances in satellite image resolution make it possible to classify multiple species with higher accuracy level (Husson et al., 2014; Ashraf and Nawaz, 2015). Recent developments in specifically designed vegetation indices for aquatic vegetation have improved identification and detection of macrophytes from medium resolution satellite images (Jiang et al., 2012; Wang et al., 2012; Villa et al., 2014; Villa et al., 2015).

Remote sensing is one of the most useful tools for mapping and studying vegetation because of the advantages of synoptic view (in time and space) compared to traditional in situ survey. Remotely sensed vegetation indices (VIs) derived from airborne and satellite images represent a powerful and effective way to monitor vegetation status, growth, and bio-physical parameters. This is especially true for aquatic ecosystems; whose characterization is extremely time-consuming and expensive. This work runs a comparison of different VIs in mapping aquatic vegetation (AV) and assesses the capabilities of three indices to analyze aquatic ecosystems: The Normalized Difference Vegetation Index (NDVI), Normalized Difference Aquatic Vegetation Index (NDAVI) and the Normalized Difference Water Index (NDWI).

2. Materials and Methods

2.1 Study Area

Lake Sevan is the largest water body in the entire South Caucasus. It is an alpine freshwater lake situated at more than 1,900 meters (6,234 ft) above sea level and is vital for Armenia's economy, tourism, agriculture, and other industrial sectors. It also has a significant cultural and recreational value for the country. The water volume and surface area of Lake Sevan have varied significantly over the past century. Since the early 1930s, Soviet authorities sought to exploit the lake to fulfill their ambitious plans for industrialization and modernization of

agriculture. It was planned to implement the project in 2 stages. In the first phase, the water level of the lake would decrease by 50 meters, and the surface of the water mirror would be reduced to seven times (Big Sevan would dry completely). In the second phase, the use of water resources to irrigate Ararat valley has been planned, as a result, the water outflow (around 700 million cubic meters per year) from the lake would be carried out. After these, about 1000 sq km of land would be vacated for agricultural purposes in the Gegharkunik region. Also, 130,000 hectares of agricultural land in Ararat Valley should be irrigated at the expense of Lake Sevan waters.

Thus, in the 1930s, the reduction of Lake Sevan had begun. During the 1st stage, the scientists recorded that the lake's ecological status suffered faster than it was supposed to be. The lake had been deprived of more than 40% of the water reserves within the next 10 years, with a maximum depth not exceeding 80 m (formerly 99 m). By the mid-1990s, the water level had decreased by around 19 meters and was subject to eutrophication, an increase in the concentration of phosphorus, nitrogen, and other plant nutrients.

In addition, the vacated areas were not suitable for agricultural use, as well as the lake's water was poorly suitable for irrigation due to the high concentration of magnesium and carbonate. There was a need to restore the lake's water reserves at the expense of other rivers being transferred to Lake Sevan. Since 1981, the Arpa-Sevan tunnel was built and part of Arpa river (South part of Armenia) water moved to the Sevan Lake.

As a result of these fluctuations in the water level in the lake, the land cover of the area has changed significantly: the coastal zones of the lake were covered with water until the 1930s, then by land after the 1930s and, finally, to this day, they continue to be covered with water (after 1981s). As of 2019, the surface area of the Sevan lake is 1 279 sq. km with 38.3 cubic km of water volume. The "blooming" of the Sevan lake was continuing to be recorded, in 2018 covering the whole lake, due to the active eutrophication processes.

2.2 Lake vegetation

Vegetation cover of the lake. Sevan has been repeatedly studied since the very beginning of hydrobiological studies on the lake (Arnoldi, 1929; Friedman, 1950; Markosian, 1951; Gambaryan, 1979). As a result of these works, the species composition of macrophytes, distribution by water area and depth, production was identified, and changes due to a decrease in the water level in the lake were also shown.

The flora of Lake Sevan basin is represented by 32 species from 27 genera and 21 families of cryptogamous and vascular macrophytes. The first ones include microscopic green (2 species: Cladophora glomerata, Enteromorpha intestinalis), yellow-green siphon (1 species pectinatus: Vaucheria dichotoma) and char (3 species: Chara globularis, C. intermedia, C. tomentosa) algae, mosses (5 species: Bryum pseudotriquetrum, Drepanocladus aduncus, Hygroamblystegium tenax, Hygrohypnum ochraceum, Schistidium cf. apocarpum), 11 species in total from 9 genera and 7 families (Ecology of Lake Sevan…, 2010).

The second group of plants is more diverse - 21 species from 18 genera and 14 families. The leading families in terms of the number of taxa are Potamogetonaceae Dumort. (3 species), Cyperaceae Juss., Lamiaceae Martinov, Lemnaceae S.F. Gray, Poaceae Barnhart, Ranunculaceae Adans. (2 types each); genus Potamogeton L. (3 species), Lemna L. (2). The water fraction (hydro-, hygro-/helo- and hydro-/hygro-helophytes) includes almost all macroalgae and mosses, with the exception of Schistidium cf. apocarpum, and 15 species from 12 genera and 11 families of vascular plants. The leading position is retained by the same families and genera, for with the exception of the families Lamiaceae, Poaceae, Ranunculaceae (Ecology of Lake Sevan…, 2010).

In the ecological spectrum, the majority of flora species (25 species, or 78.1%) belong to plants traditionally classified as aquatic. All species of macroalgae are typical hydrophytes. Almost all of the listed species of mosses are found in the waters of the lake and at considerable and even great depths.

Among the vascular plants, the most diverse are the aquatic groups: hydrophytes (10) and helophytes (5). Plants of waterlogged and humid habitats are represented by hygrophytes (6 species). The ratio of the number of hydrophytic species of vascular plants to the number of all their species is equal to 71.4% (Ecology of Lake Sevan…, 2010). It shows the specifics of the reservoir - a mountainous, deep-water lake without overgrowing coastal shallow waters, which does not allow moisture-loving coastal species to penetrate into the water.

The most common plant species (found in more than half of the parts) are Cladophora glomerata, Vaucheria dichotoma, Chara globularis, Drepanocladus aduncus, Butomus umbellatus, Myriophyllum spicatum, Potamogeton pectinatus. Enteromorpha are added on half of the segments and less intestinalis, Chara intermedia, Batrachium rionii, Bolboschoenus maritimus, Ceratophyllum demersum, Lemna gibba, L. trisulca, Phragmites australis, Potamogeton perfoliatus, Salix elbursensis, Schoenoplectus tabernaemontani, Zannichellia major. Among them are plants rare for the lake Sevan (Chara tomentosa, Bryum

pseudotriquetrum, Hygroamblystegium tenax, Hygrohypnum ochraceum, Persicaria amphibia, Phalaroides arundinacea, Potamogeton crispus, Typha angustifolia) and coastal aquatic species not typical for the lake (Schistidium cf. apocarpum, Bidens tripartita, Lycopus europaeus, Mentha caucasica, Ranunculus sceleratus).

2.3 Satellite Data Acquisition and Image Pre-Processing

Cloud free TM L2 and OLI L2 data with a resolution of 30 m were downloaded using QGIS Semi-Automatic Classification Plugin (SCP) (the path/row is 169/032 respectively). Only images with less than 10% cloud cover were selected for this study. A total of 5 OLI images and 2 TM without cloud coverage on AOI during warm season (May-September) from 2009 to 2015 were selected to ensure throughout the entire growth period of aquatic vegetation (Fig. 4).

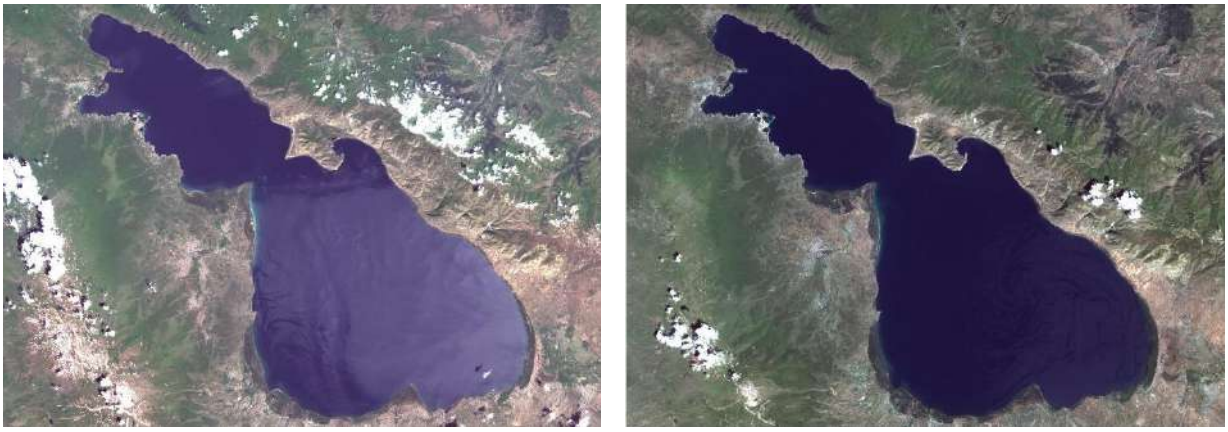

a b

Figure 3: Landsat TM and OLI images in natural color composite: a) 2011-07-28; b) 2015-06-21

All acquired images were referenced in the World Geodetic System (WGS84) datum. Details and specifications of satellite images used in this study are presented in Table 1.

Table 1. Landsat image data information

Season	Sensor	Product ID	Date
Spring	OLI/TIRS	LC08_L1TP_169032_20140517_20170422_01_T1	17.05.2014
Summer	TM	LT05_L1TP_169032_20090604_20161025_01_T1	04.06.2009

	TM	LT05_L1TP_169032_20110728_20161009_01_T1	28.07.2011
	OLI/TIRS	LC08_L1TP_169032_20130615_20170503_01_T1	15.06.2013
	OLI/TIRS	LC08_L1TP_169032_20130701_20170503_01_T1	01.07.2013
	OLI/TIRS	LC08_L1TP_169032_20150621_20170407_01_T1	21.06.2015
Autumn	OLI/TIRS	LC08_L1TP_169032_20150909_20170404_01_T1	09.09.2015

All downloaded satellite images were imported into the SCP Plugin for QGIS (Congedo, accessed 7 March, 2022). Radiance values were converted into surface reflectance based on the image-based dark object subtraction (DOS) atmospheric correction approach (Chavez, 1996) in the SCP. A radiometric correction was also applied using the semi-automatic plugin (SCP) to remove radiometric defects, haze and to improve the visual impact of true and false color composites (Fig. 4).

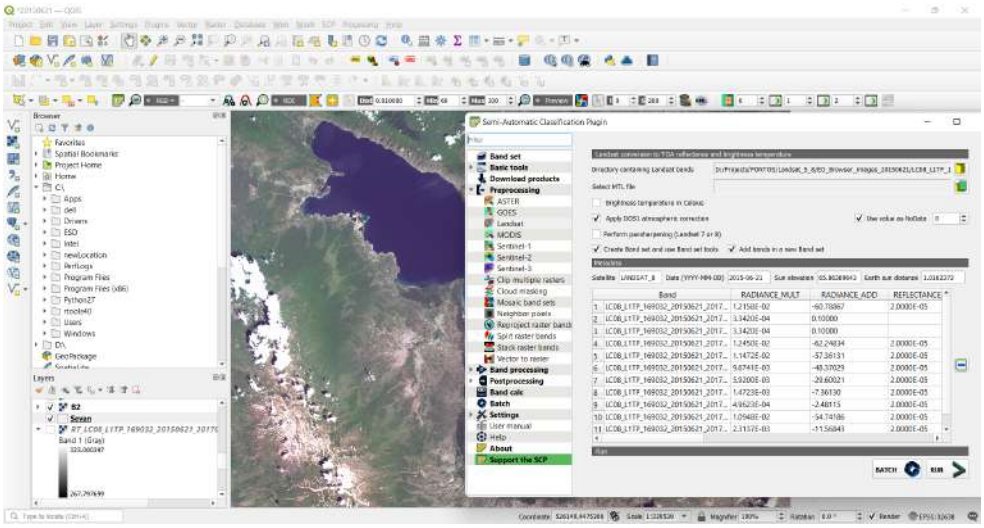

Figure 4: QGIS SCP Plugin screenshot

The lake extent with aquatic and semi-terrestrial vegetation was delineated and digitized based on visible spectral-radiometric differences in the images. The Bing Satellite Map was used for the validation. The images were clipped using the digitized polygons shapefile (Fig. 5).

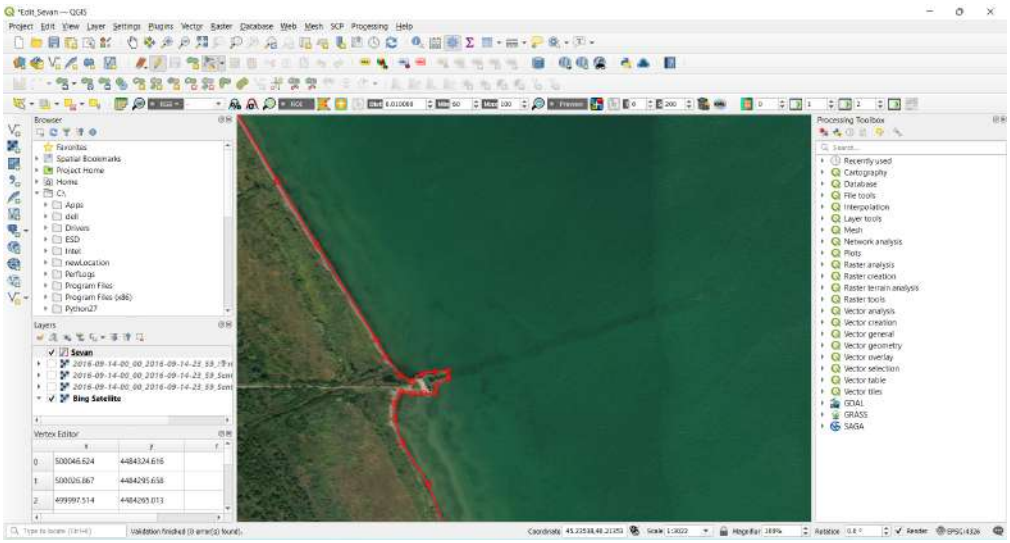

Figure 5: Lake shoreline validation on Bing satellite map

2.4 Vegetation index

Currently, it is a common method to use remote sensing data combined with various classification strategies to extract aquatic vegetation. Unfortunately, methods based on classifications need to rely on numerous measured samples to obtain satisfactory results, and such methods have proven to be inefficient (Wang et al., 2022). Therefore, scholars have attempted to design various vegetation indices that are sensitive to aquatic vegetation. In addition, many vegetation indices for identifying and enhancing aquatic vegetation based on the spectral differences of aquatic vegetation types and different sensor features have been promoted, such as the Normalized difference vegetation index (NDVI) (Klemas, 2016; Rouse et al., 1974), perpendicular vegetation index (PVI) (Richardson & Wiegand, 1977), modified normalized water index (MNDWI) (Qing, 2020), floating leaf vegetation sensitive spectral index (FVSI), planktonic algae vegetation index (floating algae index, FAI), macro aquatic vegetation index (Oyama et al., 2015; Villa et al., 2015) (Macro Algae Index, MAI), submerged aquatic vegetation sensitive spectral index (SVSI), normalized difference aquatic vegetation index (NDAVI) (Villa et al., 2014) and water adjusted vegetation index (WAVI) (Luo et al., 2016; Villa et al., 2014). Most of these involve ratios between differences and sums of the visible and near-infrared (NIR) spectral bands (Luo et al., 2017). However, the relatively weak differences in NIR band range between EAV and FAV make it difficult to further distinguish them, and also, it is difficult to eliminate the interference caused by algal blooms. Furthermore, several types of aquatic vegetation have similar spectrum curves (Hu, 2009), which makes it hard to distinguish different vegetation accurately using only the spectral index. To overcome these difficulties,

phenological features have been combined to identify various aquatic vegetation (Lei et al., 2006; Luo et al., 2016). In summary, although the existing methods can extract the aquatic vegetation above the water surface, but few methods are able to the further distinguish between EAV and FAV. In fact, it is necessary to further distinguish EAV and FAV because the dissimilar roles in water ecological environment.

Table 2. Vegetation indices for identifying aquatic vegetation.

Name/abbreviation	Formula	Reference
Normalized difference vegetation index (NDVI)	NDVI = (NIR - Red)/(NIR + Red)	(Rouse et al., 1974)
Normalized Difference Aquatic Vegetation Index (NDAVI)	NDAVI = (NIR - Blue)/(NIR + Blue)	(Villa et al., 2014)
Normalized Difference Water Index (NDWI)	NDWI = (Green – NIR)/(Green + NIR)	(McFeeters, 1996)

One of the most commonly used is the Normalized Difference vegetation Index (NDVI) which has been mostly used to capture terrestrial vegetation characteristics including growth and above ground biomass (Rouse et al., 1974). In addition to NDVI, we have applied the Normalized Difference Aquatic Vegetation Index (NDAVI) and the Normalized Difference Water Index (NDWI) which are designed to capture aquatic vegetation spectral response (McFeeters, 1996; Villa et al., 2014; Villa et al., 2015). The extracted water surfaces were also visually inspected and validated. The equations of different vegetation and water indices (Table 2) were calculated using the band calculation tool in SCP.

3. Results and Discussion

2.1 Aquatic Vegetation Extraction and Mapping

In recent years, the aquatic vegetation of Lake Sevan has experienced significant changes due to various factors.

Using the three different vegetation indices proposed in this report and the TM and OLI images to extract the annual distribution range of aquatic vegetation cover in the Lake Sevan from 2009 to 2015 (Fig.6, Annex 1), we analyzed the spatial distribution patterns and trends of aquatic.

a b c

Figure 6: Examples of the VI maps a) NDVI, b) NDAVI, c) NDWI. TM Image from 28.07.2011

As demonstrated in the figure 7, the aquatic vegetation above the water surface of Lake Sevan in case of all tree vegetation indices exhibited an overall trend of slowly from decline 2009 to 2013. A slight decrease in AW in Lake Sevan can be associated with an intensive increase in the lake level over the period 2007-2013. However, after that, the trend changes slightly. The AV demonstrates a significant upward trend in 2013 for NDAVI, but for NDVI and NDWI, the changes are insignificant in the direction of increasing.

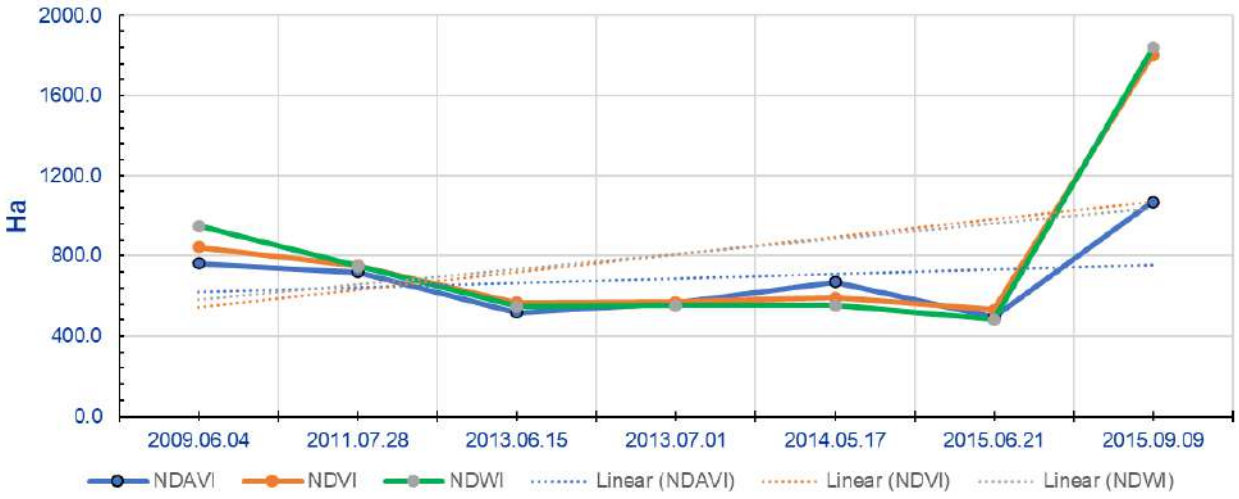

Figure 7: Dynamics of change in floating vegetation 2009-2015

Trends dropped back to 20% for all three indices in the first half of 2015. The values obtained from the 09.09.2015 OLI image are significantly different from the general trend for all three indices. For NDAVI, it increases by almost 2 times, and for NDVI and NDWI by almost 4 times. The reason for this is that the time of image capturing coincided with the blooming period of cyanobacteria. The reflectance of algal blooms in the NIR band region is similar to that of vegetation. As a result, algal bloom extracted as aquatic vegetation (Fig. 8).

Figure 8: The natural-color composite OLI image - 09.09.2015

VI values were selected from 11 random points from areas away from the coastal zone (where the concentration of aquatic vegetation is mainly observed) of lake Sevan to compare the ability of different aquatic vegetation indices to distinguish aquatic vegetation during algal blooms. Among the aquatic vegetation indices, it can be seen from the chart (Fig. 9) that NDAVI, NDVI, and NDWI have significant differences between distribution of the values. The NDAWI values are mostly distributed within the range of values that are typical for the water surface. Therefore, this index has the smallest deviation. In the case of NDVI and NDWI, the values are distributed very unevenly, but with a distinct deviation towards the ranges where vegetation is reflected.

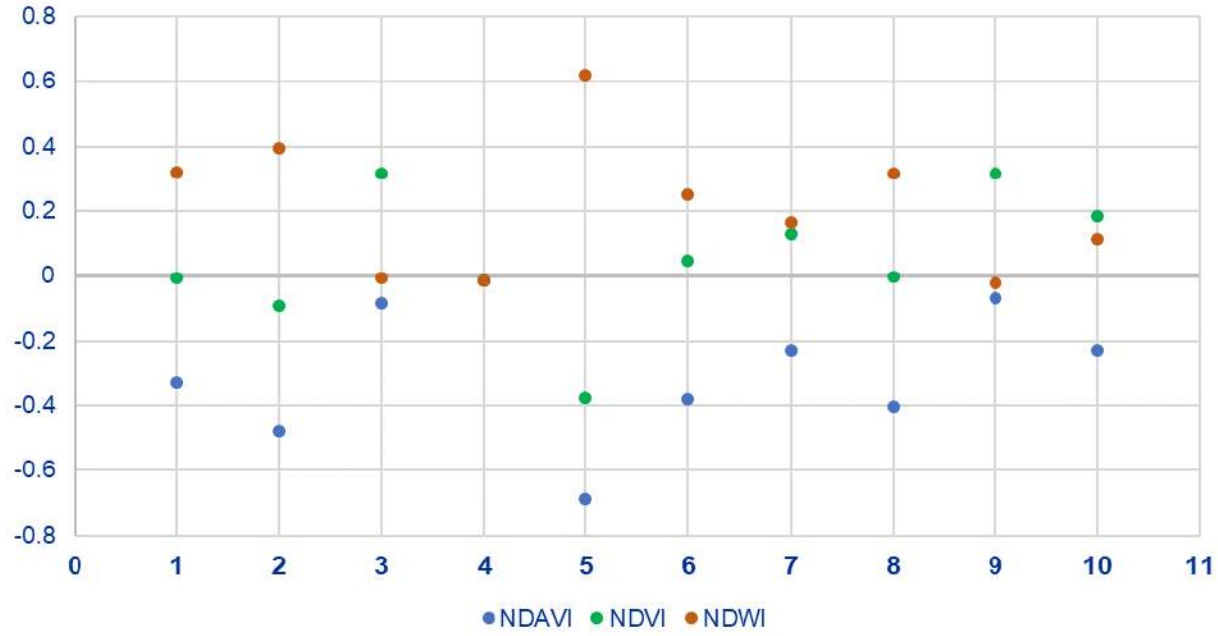

Figure 9: Distribution of values for different VIs

It worth also empathize that the algal bloom and aquatic vegetation can be accurately distinguished based on the adoption of the SWIR band. Previous studies have determined that EAV and FAV usually contain high concentrations of cellulose and lignin, which have a significant impact on the reflectance in the NIR and SWIR bands, with sensitive bands appearing at wavelengths of 930, 1,075, 1,275, 1,650, and 2,220 nm (Curran, 1989, Curran et al., 1990). Although algal contain high concentrations of chlorophyll, they almost do not contain cellulose and lignin; therefore, algal bloom present significant differences in the SWIR bands than those of EAV and FAV. Furthermore, due to the high concentration of water content in the leaf components of EAV and FAV, the reflectance exhibits a characteristic peak at the central wavelengths of 1,200, 1,450, 1,650, 1,850, and 2,015 nm (Ahamed et al., 2011, Apan et al., 2003, Galvao et al., 2005) which are not observed in the algal blooms.

2.2 Validation

Available very high-resolution (VHR) satellite imagery purchased from Maxar Technologies Inc. was used to verify the results. For the target time period, only one image tile was available for the pilot site of Armenia captured by GeoEye 1 satellite. GeoEye-1 simultaneously captures 0.41m panchromatic (black & white) and 1.65m multispectral (colour) digital imagery. It has 5 spectral band - Pan: 450-800 nm; Blue: 450-510 nm; Green: 510-580 nm; Red: 655-690 nm and Near IR: 780-920 nm. Overall accuracy is estimated < 3m CE90 at nadir. The used image was

captured on August 02, 2014 (Fig. 10). The area is the north-west coast of the Lake Sevan between Sevan town and Norashen village.

Figure 10: GeoEye 1 image (Image ID: 10504100111C5400) in natural color composition

Landsat OLI image dated August 12, 2014 was chosen for comparative analysis. Landsat OLI image extracted by GeoEye-1 image borders.

The statistical comparison of vegetation index maps shows that Landsat images provide up to 65-70% of the result of GeoEye-1 images for highlighting aquatic vegetation (Fig. 11). Considering the fact that the resolution of Landsat images is about 18 times smaller, we think that this figure is quite high a suck kind research.

This also indicates that Landsat images, although not suitable for studies that require high detailization (in particular, to determine the species composition of aquatic vegetation), but can provide sufficiently high-precision results for assessing the dynamics of changes in objects and phenomena over time.

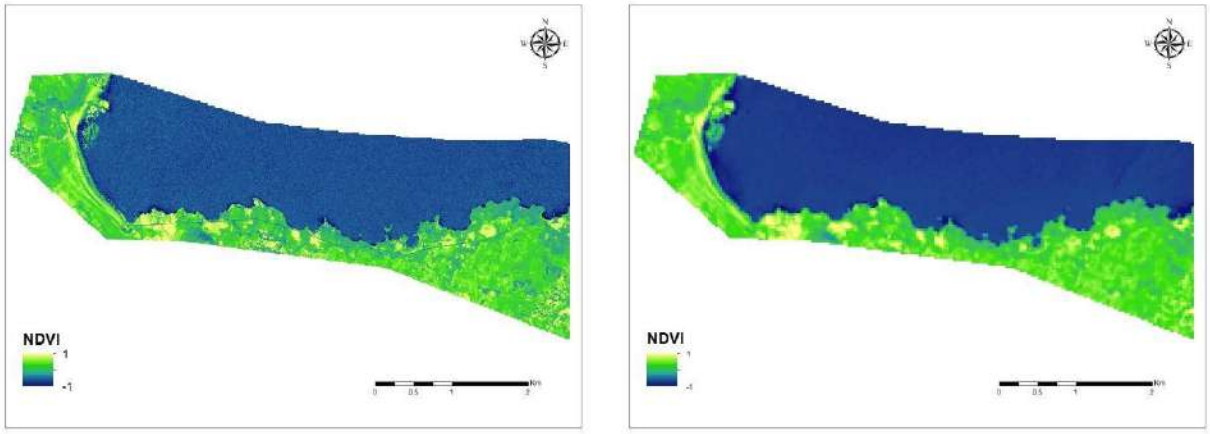

a b

Figure 11: Visual Comparison of NDVI Maps of the North-Western Shore of Lake Sevan: a) GeoEye-1, b) Landsat OLI

2.3 Wetland Extraction and Mapping

A combination of supervised (ISO Cluster Unsupervised Classification) and supervised (Maximum Likelihood) classification based on NDVI was used to extract and map wetlands in the Lake Sevan basin. Classification was applied with a total of 3 classes – water, vegetation and other. Field work was carried out to validate and collect ground data. Although we must admit that the locations of the wetlands in the basin were known from the beginning and the results of the classification revealed exactly those places that were known (Fig. 12). The total area of wetlands in the area adjacent to Lake Sevan is about 60 ha and has not changed much over the years.

Fig. 12 An example of a water-swamp bodies, in the area adjacent to Lake Sevan, near the town of Martuni. Basemap - Bing Satellite

4. Ground Truthing

Two ground inspection missions were carried out in the lake basin for the proper validation and evaluation the laboratory analyzes results.

Two wetland areas (near Lichk and Noratus) and a lagoon near Norashen with growing aquatic vegetation have been visiting during the first field visit (09.09.2021). Four pre-determined points were visited during the second mission near (1) Martuni, (2) Hayrivank, (3) Norashen Reserve and (4) near the mouth of the Dzknaget River for the visual observation and photographing (Fig. 11).

Figure 11: Areas in the Lake Sevan basin visited for ground truthing. Basemap - OpenStreetMap

The main purpose of the visit was to study the species composition of aquatic vegetation, as well as to find out at the Dzknaget estuary whether the biomass distinguished from the satellite imagery is really aquatic vegetation or tree coexistence left in the water as a result of the level rise.

The observations and data collected in the field were used in the process of further adjustment of the results of the analysis.

5. Conclusion

This study showed the use of remote sensing imagery with field data to explore the long-term spatio-temporal changes of aquatic vegetation in Lake Sevan. The overall moderate output was obtained from a moderate-resolution image and different vegetation index analyses. Therefore, the results obtained in this study indicated the potential of freely available medium-resolution Landsat and similar satellite images to monitor the Spatio-temporal changes of lakes in a reproducible and continuous manner. The results also show that a decrease in the long-term water level in the lake favors the spread of macrophytes. It can also be assumed that the dynamics of changes in the cover of aquatic vegetation in Lake Sevan, along with long-term fluctuations in water level, are also associated with strong anthropogenic disturbances. It should also be emphasized that the aquatic vegetation of Lake Sevan, which is more or less accurately

distinguished on the maps of vegetation indices obtained from medium-resolution satellite images, is mainly represented by EAV, which generally grows in the coastal zone, and not in deep lagoons. Dominant species are Butomus umbellatus and Potamogeton pectinatus.

One of the most important findings of the study is that algal blooms can be a huge barrier to correctly detecting aquatic vegetation from satellite imagery. This problem will be especially relevant in cases where the extraction will be based on automatic and semi-automatic machine learning algorithms. Thus, an additional solution should be applied to avoid this. Our recommendation is to avoid using images captured during the blooming season (mid-summer to mid-autumn), or to use more in-depth scientific approaches, in particular develop algorithms based on the adoption of the SWIR band.

Acknowledgments

The research was financially supported by “Copernicus assisted environmental monitoring across the Black Sea Basin-PONTOS” project funded by the European Union’s ENI CBC Black Sea Basin Programme 2014-2020. We are especially grateful to colleagues from partner institutions for their comprehensive assistance in various stages of the study.

References

1. Ahamed, T., Tian, L., Zhang, Y., Ting, K.C., 2011. A review of remote sensing methods for biomass feedstock production. Biomass Bioenergy 35 (7), 2455–2469. https://doi.org/10.1016/j.biombioe.2011.02.028.
2. Alahuhta, J.; Kanninen, A.; Vuori, K.-M. Response of macrophyte communities and status metrics to natural gradients and land use in boreal lakes. Aquat. Bot. 2012, 103, 106–114.
3. Albright, T.P.; Ode, D.J. Monitoring the dynamics of an invasive emergent macrophyte community using operational remote sensing data. Hydrobiologia 2011, 661, 469–474.
4. Apan, A., Held, A., Phinn, S., Markley, J., 2003. Formulation and assessment of narrow-band vegetation indices from EO-1 Hyperion imagery for discriminating sugarcane disease. In: Proceedings of the Spatial Sciences Institute Biennial Conference (SSC 2003): Spatial Knowledge Without Boundaries, pp. 1–13.
5. Arnoldi L.V. Materials on the study of the bottom productivity of Lake Sevan // Tr. SGBS /

Ed. M.A. Fortunatov. Erivan: Armpolygraph, 1929. V. 2, I 1.

6. Ashraf, M.; Nawaz, R. A comparison of change detection analyses using different band algebras for baraila wetland with Nasa's multi-temporal Landsat dataset. Int. J. Geogr. Inf. Syst. 2015, 7, 1.
7. Beck, M.W.; Hatch, L.K.; Vondracek, B.; Valley, R.D. Development of a macrophyte-based index of biotic integrity for Minnesota lakes. Ecol. Indic. 2010, 10, 968–979. [CrossRef]
8. Birk, S.; Ecke, F. The potential of remote sensing in ecological status assessment of coloured lakes using aquatic plants. Ecol. Indic. 2014, 46, 398–406.
9. Burlakoti, C.; Karmacharya, S.B. Quantitative analysis of macrophytes of Beeshazar Tal, Chitwan, Nepal. *H. J. Sci.* **2004**, *2*, 37–41.
10. Chambers, P.; Lacoul, P.; Murphy, K.; Thomaz, S. Global diversity of aquatic macrophytes in freshwater. In *Freshwater Animal Diversity Assessment*; Springer: Berlin, Germany, 2007; pp. 9–26.
11. Chappuis, E.; Gacia, E.; Ballesteros, E. Environmental factors explaining the distribution and diversity of vascular aquatic macrophytes in a highly heterogeneous Mediterranean region. Aquat. Bot. 2014, 113, 72–82.
12. Chavez, P.S. Image-based atmospheric corrections-revisited and improved. Photogramm. Eng. Remote Sens. 1996, 62, 1025–1035
13. Congedo, L. Semi-Automatic Classification Plugin Documentation. Available online: https://fromgistors.blogspot.com/p/semi- automatic-classification-plugin.html (accessed on 7 March 2022).
14. Curran, P.J., 1989. Remote sensing of foliar chemistry. Remote Sens. Environ. 30 (3), 271–278. https://doi.org/10.1016/0034-4257(89)90069-2.
15. Curran, P.J., Dungan, J.L., Gholz, H.L., 1990. Exploring the relationship between reflectance red edge and chlorophyll content in slash pine. Tree Physiol. 7 (1–2-3–4), 33–48. https://doi.org/10.1093/treephys/7.1-2-3-4.33.
16. Damtew, Y.T.; Verbeiren, B.; Awoke, A.; Triest, L. Satellite Imageries and Field Data of Macrophytes Reveal a Regime Shift of a Tropical Lake (Lake Ziway, Ethiopia). Water 2021, 13, 396. https://doi.org/10.3390/w13040396
17. Dolinar, N.; Regvar, M.; Abram, D.; Gaberščˇik, A. Water-level fluctuations as a driver of

Phragmites australis primary productivity, litter decomposition, and fungal root colonisation in an intermittent wetland. *Hydrobiologia* **2016**, *774*, 69–80.

18. Ecology of Lake Sevan During the Period of Water Level Rise. The Results of Russian-Armenian Biological Expedition for Hydroecological Survey of Lake Sevan (Armenia) (2005–2009). Makhachkala: Nauka DNT, 2010. 348 p. ISBN 978-5-94434-162-4.
19. Engelhardt, K.A.; Ritchie, M.E. Effects of macrophyte species richness on wetland ecosystem functioning and services. *Nature* **2001**, *411*, 687–689.
20. Fridman G.M. Bottom fauna of Lake Sevan // Tr. SGBS. 1950, vol. 11, pp. 7–92.
21. Galvao, L.S., Formaggio, A.R., Tisot, D.A., 2005. Discrimination of sugarcane varieties in Southeastern Brazil with EO-1 Hyperion data. Remote Sens. Environ. 94 (4), 523–534.
22. Gambaryan P.P. Distribution of macrophytes of Lake Sevan // Tr. SGBS. 1979, vol. 17, pp. 123–129.
23. García-Girón, J.; Fernández-Aláez, C.; Fernández-Aláez, M.; Alahuhta, J. Untangling the assembly of macrophyte metacommuni- ties by means of taxonomic, functional and phylogenetic beta diversity patterns. Sci. Total Environ. 2019, 693, 133616.
24. H. Wang, Y. Li, Sh. Zeng, X. Cai, Sh. Bi, H. Liu, M. Mu, X. Dong, J. Li, J. Xu, H. Lyu, Y. Zhu, Yu Zhang. 2022. Recognition of aquatic vegetation above water using shortwave infrared baseline and phenological features. Ecological Indicators. Vol. 136, https://doi.org/10.1016/j.ecolind.2022.108607
25. Hu, C., 2009. A novel ocean color index to detect floating algae in the global oceans. Remote Sens. Environ. 113 (10), 2118–2129.
26. Hunter, P.; Gilvear, D.; Tyler, A.; Willby, N.; Kelly, A. Mapping macrophytic vegetation in shallow lakes using the Compact Airborne Spectrographic Imager (CASI). *Aquat. Conserv. Mar. Freshw. Ecosyst.* **2010**, *20*, 717–727.
27. Husson, E.; Hagner, O.; Ecke, F. Unmanned aircraft systems help to map aquatic vegetation. Appl. Veg. Sci. 2014, 17, 567–577.
28. Jakubauskas, M.; Kindscher, K.; Fraser, A.; Debinski, D.; Price, K. Close-range remote sensing of aquatic macrophyte vegetation cover. Int. J. Remote Sens. 2000, 21, 3533–3538.

29. Jiang, H.; Zhao, D.; Cai, Y.; An, S. A method for application of classification tree models to map aquatic vegetation using remotely sensed images from different sensors and dates. Sensors 2012, 12, 12437–12454. [CrossRef]

30. Junk, W.; Howard-Williams, C. Ecology of aquatic macrophytes in Amazonia. In the Amazon; Springer: Berlin, Germany, 1984; pp. 269–293.

31. Klemas, V.V., 2016. Remote Sensing of Submerged Aquatic Vegetation. Springer International Publishing.

32. La Toya, T.K.; Jacob, D.L.; Hanson, M.A.; Herwig, B.R.; Bowe, S.E.; Otte, M.L. Macrophytes in shallow lakes: Relationships with water, sediment and watershed characteristics. *Aquat. Bot.* **2013**, *109*, 39–48.

33. Lawniczak, A.; Zbierska, J.; Choin´ski, A.; Szczepaniak, W. Response of emergent macrophytes to hydrological changes in a shallow lake, with special reference to nutrient cycling. Hydrobiologia 2010, 656, 243–254.

34. Lei, Z., Delan, X.U., Huang, P., Pan, H., Wang, B., Liu, Z., University, J., Guangzhou, & China, 2006. Submersed and floating-leaved macrophytes in Taihu Lake and their water environmental effect. Ecol. Environ. https://doi.org/10.1111/j.1744- 7917.2006.00098.x.

35. Lindholm, M.; Alahuhta, J.; Heino, J.; Hjort, J.; Toivonen, H. Changes in the functional features of macrophyte communities and driving factors across a 70-year period. Hydrobiologia 2020, 847, 3811–3827.

36. Luo, F.-L.; Jiang, X.-X.; Li, H.-L.; Yu, F.-H. Does hydrological fluctuation alter impacts of species richness on biomass in wetland plant communities? *J Plant Ecol* **2016**, *9*, 434–441.

37. Luo, J., Duan, H., Ma, R., Jin, X., Li, F., Hu, W., Shi, K., Huang, W., 2017. Mapping species of submerged aquatic vegetation with multi-seasonal satellite images and considering life history information. Int. J. Appl. Earth Obs. Geoinf. 57, 154–165.

38. Luo, J., Li, X., Ma, R., Li, F., Duan, H., Hu, W., Qin, B., Huang, W., 2016a. Applying remote sensing techniques to monitoring seasonal and interannual changes of aquatic vegetation in Taihu Lake, China. Ecol. Indic. 60, 503–513.

39. Luo, J., Ma, R., Feng, H., Li, X., 2016b. Estimating the Total Nitrogen Concentration of Reed Canopy with Hyperspectral Measurements Considering a Non-Uniform Vertical Nitrogen Distribution. Remote Sensing 8 (10), 789. https://doi.org/10.3390/rs8100789.

40. Markosyan A.G. Distribution and biomass of charophytes and moss in Lake Sevan // Tr. SGBS. 1951, vol. 12, pp. 29–33.

41. McFeeters, S.K. The use of the Normalized Difference Water Index (NDWI) in the delineation of open water features. Int. J. Remote Sens. 1996, 17, 1425–1432.

42. Ou, K., Lin, H., Cui, G., Xia, W., 2008. Emergent plants and their garden applications. J. Anhui Agric. Sci. 36 (20), 8556–8558.

43. Oyama, Y., Matsushita, B., Fukushima, T., 2014. Distinguishing surface cyanobacterial blooms and aquatic macrophytes using Landsat/TM and ETM+ shortwave infrared bands. Special Issue: Remote Sens. Inland Waters 157, 35–47. https://doi.org/10.1016/j.rse.2014.04.031.

44. Qing, S, Runa, A., Shun, B., et al., 2020. Distinguishing and mapping of aquatic vegetations and yellow algae bloom with Landsat satellite data in a complex shallow Lake, China during 1986–2018. Ecol. Indic. 112, 106073.

45. Richardson, A.J., Wiegand, C.L., 1977. Distinguishing vegetation from soil background information. Pe & Rs 43 (12).

46. Rivera, S.; Landom, K.; Crowl, T. Monitoring macrophytes cover and taxa in Utah Lake by using 2009–2011 Landsat digital imagery. Rev. De Teledetección 2013, 39, 106–115.

47. Rouse, J.; Haas, R.; Schell, J.; Deering, D. Monitoring vegetation systems in the Great Plains with ERTS. In Third Earth Resources Technology Satellite-1. Dec. Goddard Space Flight Cent. NASA 1974, 351, 309–317.

48. Seddon, B. Aquatic macrophytes as limnological indicators. Freshwat. Biol. 1972, 2, 107–130.

49. Tan, W.; Xing, J.; Yang, S.; Yu, G.; Sun, P.; Jiang, Y. Long Term Aquatic Vegetation Dynamics in Longgan Lake Using Landsat Time Series and Their Responses to Water Level Fluctuation. Water 2020, 12, 2178.

50. Thomaz, S.; Esteves, F.; Murphy, K.; Dos Santos, A.; Caliman, A.; Guariento, R. Aquatic macrophytes in the tropics: Ecology of populations and communities, impacts of invasions and human use. *Trop. Biol. Conserv. Manag.* **2009**, *4*, 27–60.

51. Triest, L.; Sierens, T.; Terer, T. Diversity and fine-scale spatial genetic structure of Cyperus papyrus populations in Lake Naivasha (Kenya) using microsatellite markers. Hydrobiologia 2014, 737, 131–144.

52. Van Geest, G.; Coops, H.; Roijackers, R.; Buijse, A.; Scheffer, M. Succession of aquatic vegetation driven by reduced water-level fluctuations in floodplain lakes. *J. Appl. Ecol.* **2005**, *42*, 251–260.

53. Villa, P.; Bresciani, M.; Bolpagni, R.; Pinardi, M.; Giardino, C. A rule-based approach for mapping macrophyte communities using multi-temporal aquatic vegetation indices. Remote Sens. Environ. 2015, 171, 218–233.

54. Villa, P.; Bresciani, M.; Braga, F.; Bolpagni, R. Comparative assessment of broadband vegetation indices over aquatic vegetation. IEEE J. Sel. Top. Appl. 2014, 7, 3117–3127.

55. Vis, C.; Hudon, C.; Carignan, R. An evaluation of approaches used to determine the distribution and biomass of emergent and submerged aquatic macrophytes over large spatial scales. Aquat. Bot. 2003, 77, 187–201.

56. Wang, L.; Dronova, I.; Gong, P.; Yang, W.; Li, Y.; Liu, Q. A new time series vegetation–water index of phenological–hydrological trait across species and functional types for Poyang Lake wetland ecosystem. Remote Sens. Environ. 2012, 125, 49–63.

57. Zhang, Y.; Liu, X.; Qin, B.; Shi, K.; Deng, J.; Zhou, Y. Aquatic vegetation in response to increased eutrophication and degraded light climate in Eastern Lake Taihu: Implications for lake ecological restoration. *Sci. Rep.* **2016**, *6*, 1–12.

58. Zhu, J.; Deng, J.; Zhang, Y.; Peng, Z.; Hu, W. Response of Submerged Aquatic Vegetation to Water Depth in a Large Shallow Lake after an Extreme Rainfall Event. Water 2019, 11, 2412.

Annex 1. NDVI time series in nearby Hayravank monastery

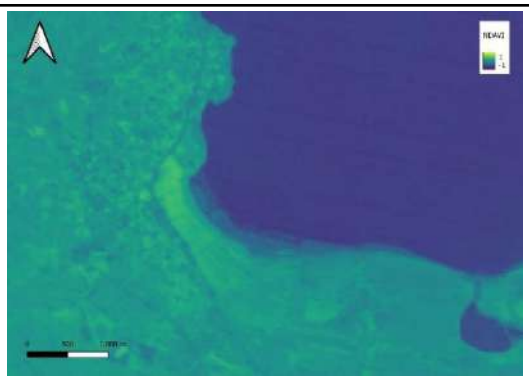

2009-06-04

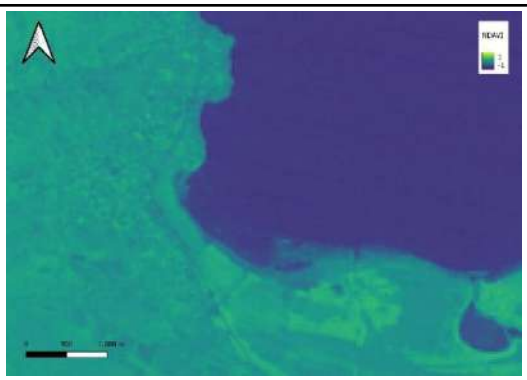

2011-07-28

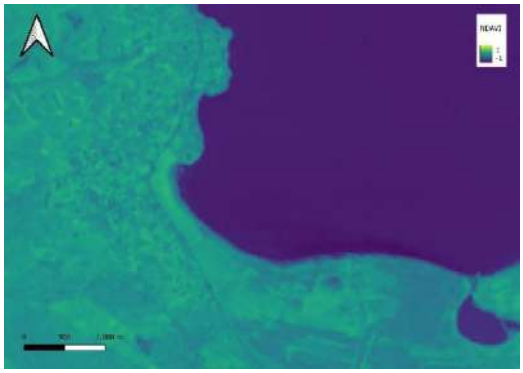

2013-06-15

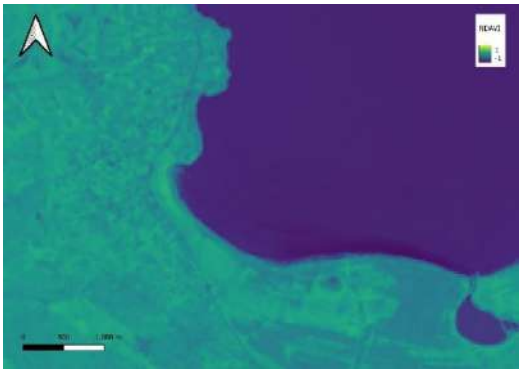

2013-07-01

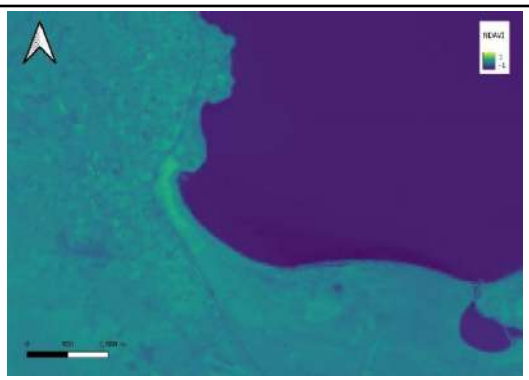

2014-05-17

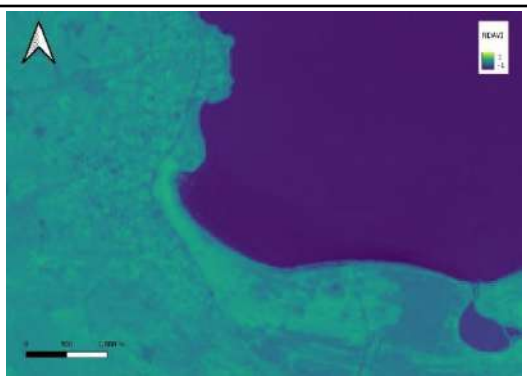

2015-06-21

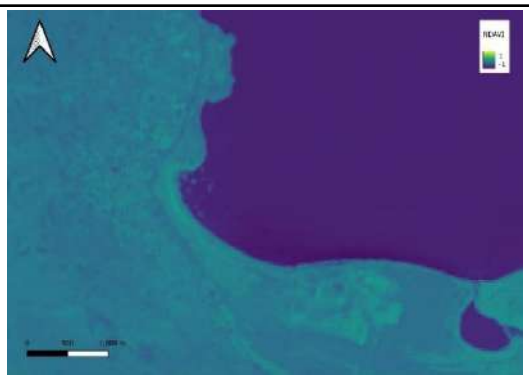

2015-09-09

Annex 2 Photos from the ground truthing


Photos from 09.09.2021. Wetlands near Lichk


Photos from 09.09.2021. Wetlands near Noratus


Photos from 19.07.2022. Aquatic vegetation near Martuni


Photos from 19.07.2022. Aquatic vegetation near Hayrivank


Photos from 19.07.2022. Aquatic vegetation near Norashen Reserv

Photos from 19.07.2022. A mixture of aquatic vegetation and trees left in the water after level rise near River Dzknaget Mouth